EUROFUSION WPMAG-CP(16) 15044

K Sedlak et al.

Thermal-Hydraulic and Quench Analysis of the DEMO Toroidal Field Winding Pack WP1

Preprint of Paper to be submitted for publication in Proceedings of 29th Symposium on Fusion Technology (SOFT 2016)

This work has been carried out within the framework of the EUROfusion Consortium and has received funding from the Euratom research and training programme 2014-2018 under grant agreement No 633053. The views and opinions expressed herein do not necessarily reflect those of the European Commission.

Thermal-Hydraulic and Quench Analysis of the DEMO Toroidal Field Winding Pack WP1

Kamil Sedlak[a], Pierluigi Bruzzone[a], Monika Lewandowska[b]

[a]*École Polytechnique Fédérale de Lausanne (EPFL), Swiss Plasma Center, 5232 Villigen PSI, Switzerland*
[b]*West Pomeranian University of Technology, Szczecin, Poland*

Three alternative designs of the toroidal field (TF) coil were proposed for the European DEMO being developed under the Eurofusion Consortium. The most ambitious TF coil winding pack in terms of technological deviation from the ITER TF coil design and consequent potential cost saving, the so-called WP1, is based on the react&wind technology of Nb_3Sn layer-wound flat multistage conductors. We present the thermal-hydraulic and quench propagation analyses for the WP1 proposed in 2015, in which the realistic magnetic field and nuclear heat load maps are taken into account. The aim of the analysis, performed using the Cryosoft software, is to assess the temperature margin at the end-of-burn conditions, as well as the hot-spot temperature that is expected in case of quench, and consequently to optimize the WP1 design from the thermal-hydraulic point of view.

Keywords: DEMO, toroidal field coil, thermal analysis, hydraulic analysis, quench, heat transfer.

1. Introduction

The European DEMO fusion tokamak is being designed as a machine that will follow ITER reactor. The aim of DEMO is to demonstrate feasibility of electricity production, which has two consequences – firstly, the size of the device will be significantly larger than that of ITER, secondly, an emphasis is put on the cost efficiency of the employed technologies.

One of the main DEMO components is the toroidal field (TF) coil system, consisting of 18 identical coils [1]. The TF winding pack (WP) and conductor is being designed in four parallel versions – one of them is based on the high temperature superconductors, the other three on more conventional low temperature superconductors (LTS), namely Nb_3Sn and NbTi. One of the three LTS concepts, called RW1 design, is based on the layer-winding and react&wind technology. The latest update of the RW1 design is described in [2], and the presented analysis is based on it. The present analysis is based on the latest update of the RW1 design [2], extending the earlier thermal-hydraulic studies [3]-[6] based on the previous TF WP design. Recent thermal-hydraulic analyses of the other two LTS WP concepts are presented in [6]-[8].

2. Conductor Design

The DEMO TF winding pack RW1 is a layer wound coil [2], where every layer is graded, i.e. the amount of superconductor, copper, helium and steel varies from layer to layer depending on the magnetic field, nuclear heat load and mechanical electromagnetic load in a given layer. From a hydraulic point of view, the layers form parallel branches of the WP cooling circuit. The scheme of the cooling circuit can be found in [9].

The react&wind Nb_3Sn conductor is presented in Fig. 1 and described in detail in [2]. In the following we just summarize the main characteristics of the conductor relevant for the thermal-hydraulic analysis.

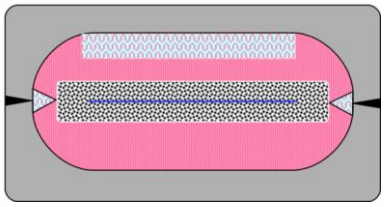

Fig. 1. React&wind conductor for the first layer of the DEMO TF coil.

The conductor consists of a flat two-stage fully-transposed cable (19 strands in the first stage; 14 first-stage subcables in the bundle), a solid composite stabilizer made of 95% Cu and 5% CuNi, two triangular and one rectangular helium cooling channels, and a steel conduit longitudinally welded around the conductor assembly. The boundary between Cu/CuNi stabilizer and the steel conduit is not tight, allowing helium exchange between the cable bundle and all three cooling channels. Helium flow is enforced by the pressure drop of 1 bar over the conductor length, with inlet pressure of 6 bar and outlet pressure of 5 bar. Helium inlet temperature is 4.5 K.

3. Thermo-Hydraulic Model

The thermo-hydraulic behavior of the conductor is investigated by the program Thea [10] from Cryosoft. The conductor is modelled as a 1-D system of several parallel components – three thermal components (strands, Cu/CuNi stabilizer and steel jacket) and three hydraulic components (He in the bundle, He in the triangular side cooling channels, and He in the upper

author's email: kamil.sedlak@psi.ch

rectangular channel). The friction correlation in the bundle region is based on the Darcy-Forchheimer equation [11], the friction correlations in the cooling channels in the turbulent regime are given by the Bhatti-Shah correlation [12]. Heat transfer h between the solid components is set to 500 W/(m^{2}K) [13], where the contact surface between strands and copper stabilizer is assumed to be 1/5 of the overall boundary area. Heat transfer between helium and solid components, h_{st}, in turbulent flow is driven by the Dittus-Boelter correlation [13]. The details concerning the friction correlations and heat transfer coefficients in laminar regime are specified in [13]. Fig. 2 illustrates the heat-exchange links between the individual components.

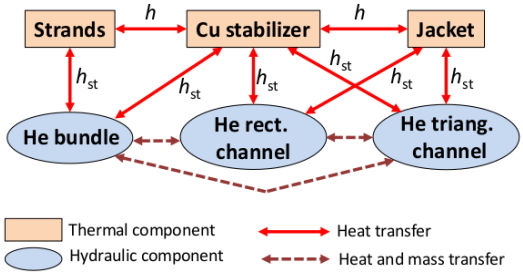

Fig. 2. Heat and mass exchange between the thermal and hydraulic components in the Thea model of RW1 conductor.

We experienced a numerical problem in Thea when helium exchange was allowed between all three channels simultaneously. As a work-around solution, the helium exchange was enabled between two hydraulic components at a given element n (e.g. bundle and upper channel), between different two components at the neighboring element n+1 (e.g. bundle and triangular channels), and between yet another two components at element n+2 (e.g. upper channel and triangular channels). This helium-exchange pattern was repeated along the full conductor length. This way the numerical problem was resolved, while helium exchange between all components was allowed.

Table 1. Nuclear heat load (NHL), outlet temperature (T_{out}), total mass flow rate (dm/dt), maximum effective field B_{eff} and minimum quench energy (MQE) in individual layers.

Layer	NHL (W)	T_{out} (K)	dm/dt (g/s)	max B_{eff} (T)	MQE (J)
1	36.1	5.10	18.3	12.26	3.4
2	28.1	5.00	18.3	11.21	5
3	22.6	4.95	18.3	10.4	7
4	18.3	4.92	15.6	9.75	15
5	14.7	4.92	14.9	8.88	30
6	11.8	4.90	12.2	8.19	50
7	9.3	4.89	10.9	7.47	115
8	7.3	4.87	8.9	6.93	350
9	5.3	4.84	7.6	6.74	720
10	4.2	4.81	6.4	6.58	430
11	3.3	4.78	5.1	6.46	500
12	1.7	4.74	5.4	6.14	65

4. Quench Calculations

The quench simulations were done on individual conductor layers, not taking into account heat transfer from layer to layer and from turn to turn. Magnetic field distribution along each conductor length was calculated using program M'C from Cryosoft.

First of all, a steady-state situation is modelled, in which nuclear heat load (e.g. 36.1 W in layer 1) is deposited along the layer, and ohmic heating at the joint (2 W per layer) is generated at the initial 0.5 m of the conductor [14]. Mass flow rate, outlet temperature and some other variables for each layer are presented in Table 1. The steady-state is subsequently used as the initial state for the quench calculations.

The quench is initiated by heating a 10 cm long initiation zone located somewhere near the conductor center, to avoid any edge-effects that might occur near the conductor edge, at the location of local maximum of the temperature margin. The quench initiated in the region of highest temperature margin is going to propagate slowest, and is therefore expected to lead to the highest hot-spot temperature, and becomes the worst-case (though the least likely) quench scenario.

The spatial adaptive mesh was used in Thea. The adaptive meshing is triggered wherever the temperature exceeds 6 K, with the minimum mesh size of 1 cm. Regardless of the temperature, a fine mesh of 5 cm long elements is set right from the beginning of the simulation in the region 5 m before and 5 m after the quench initiation zone. In the rest of the conductor (~840 m in case of layer 1), the initial element size is set to 1 m.

The quench evolution in the layer 1, where effective magnetic field of up to 12.2 T [2] is the highest one, is presented in Fig. 3. and 4.

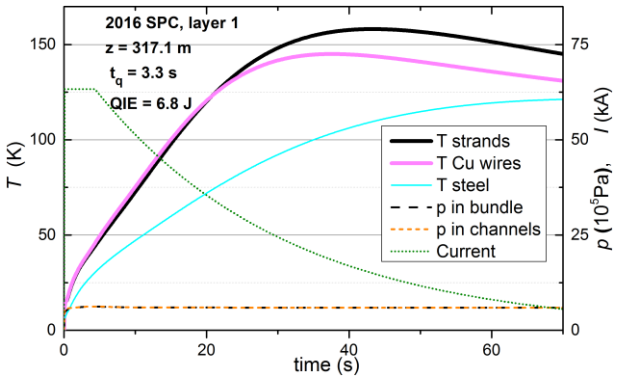

Fig. 3. Quench evolution in the conductor of layer 1 of the SPC RW1 coil simulated with Thea. Temperature and pressure is calculated at the hot spot location at z = 317.1 m.

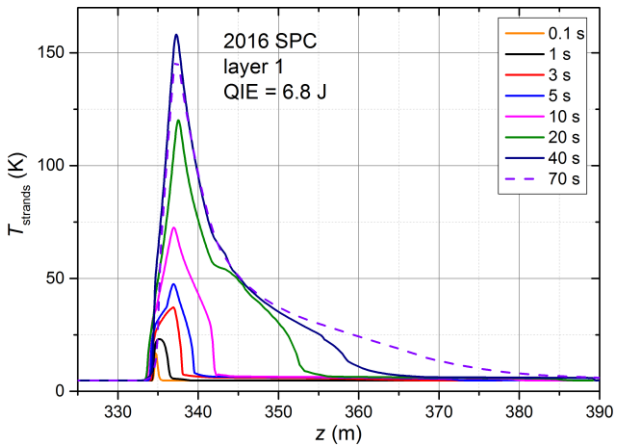

Fig. 4. Quench propagation along the conductor length.

The quench initiation energy (QIE) was set two times higher than the minimum quench energy (MQE), and was deposited at the beginning of the simulation over the period of time of 0.1 s [8]. After the quench initiation, the resistive voltage over the full conductor length was gradually rising. After 3.3 s, the voltage exceeded the quench detection voltage threshold, V_{thr}, of 0.1 V. The operating current of 63.3 kA remained at the nominal value for another 1.1 s, corresponding to the quench validation time (0.1 s) and breakers opening (1.0 s), and afterwards decayed exponentially with the decay constant of 27 s.

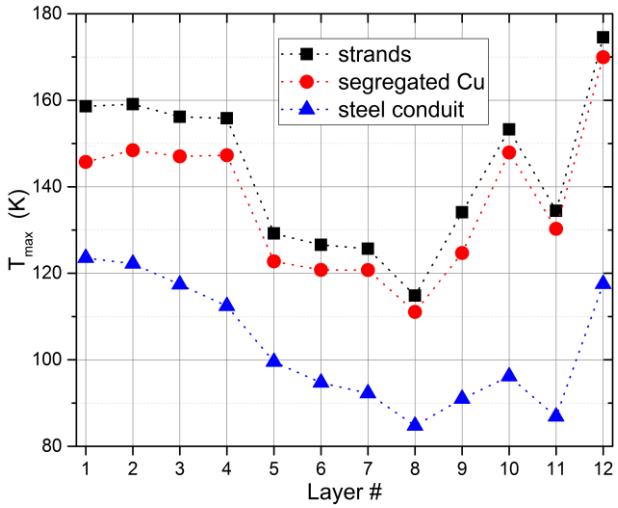

Fig. 5. Hot-spot temperature in different thermal components of each layer.

ddd

Quenches in all layers were investigated. The MQE differs enormously, and spans from 3.4 J in layer 1 up to 720 J in layer 11. Also the time of voltage rise up to the V_{thr} differs significantly, the shortest being 3.3 s in layer 1, the longest 13.9 s in layer 10. The hot-spot temperatures in all layers are shown in Fig. 5. The steel temperature stays always below 150 K criterion specified for DEMO in [14]. The strand temperature remains below 180 K.

Figure 6 illustrates the dependence of the hot-spot temperature on the quench detection voltage threshold. The value of V_{thr} used to be set to 0.5 V in the earlier DEMO studies [3]-[8]. This value was probably too conservative, and in 2016 the threshold was therefore reduced [14] to the value used by ITER, i.e. 0.1 V.

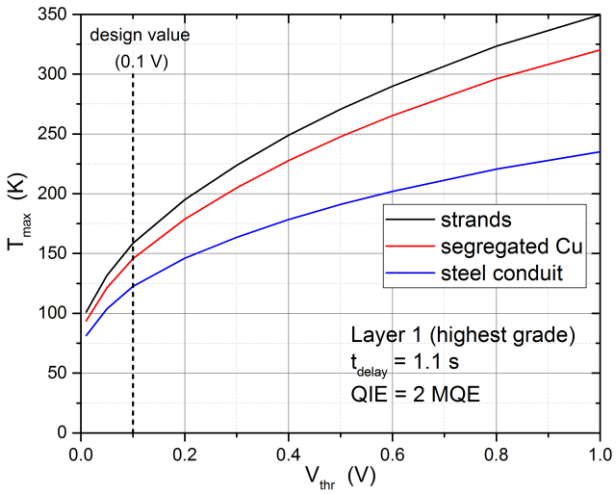

Fig. 6. Dependence of hot-spot temperature in layer 1 on the quench detection threshold voltage V_{thr}. The nominal value used in DEMO is $V_{thr} = 0.1$ V.

Another important parameter affecting the hot-spot temperature is the delay time between the moment when voltage exceeds V_{thr} and the breakers opening. The effect of the delay time is presented in Fig. 7. Also the nominal delay time has been reduced in 2016 to 1.1 s [14], compared to 2.0 s used in the previous years.

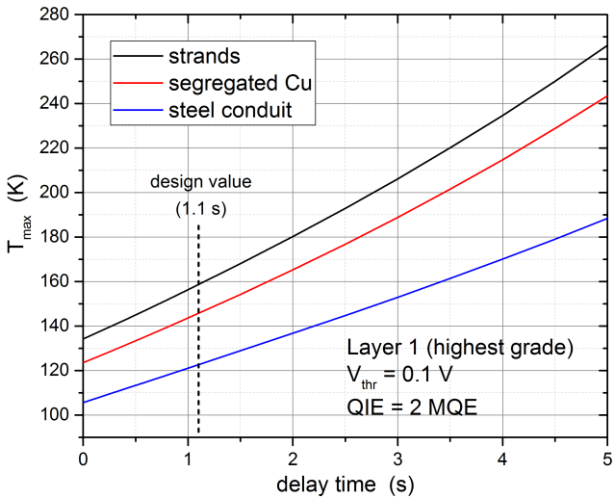

Fig. 7. Dependence of hot-spot temperature in layer 1 on the delay time between the quench voltage threshold is exceeded and the current dump initiated.

Figure 8 indicates that the hot-spot temperature is very weakly dependent on the quench initiation energy.

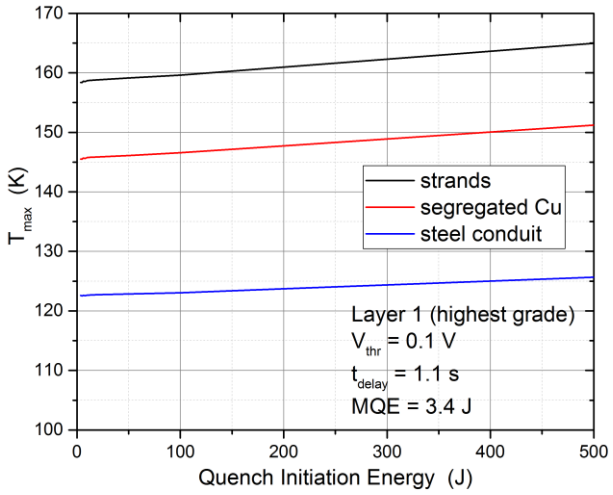

Fig. 8. Dependence of hot-spot temperature in layer 1 on the quench initiation energy.

It can be expected that quench that is initiated very locally, e.g. due to a local conductor damage, will lead to a higher hot-spot temperature compared to the quench initiated over a longer conductor length. In the former case, the normal resistive zone is initially very short, and a longer time is required to detect the quench and initiate the current dump, which might lead to higher hot-spot temperature locally in the quench initiation zone. Though this effect is confirmed by Thea calculations shown in Fig. 9, there is some saturation of the hot-spot temperature for initiation zones shorter than 0.5 m.

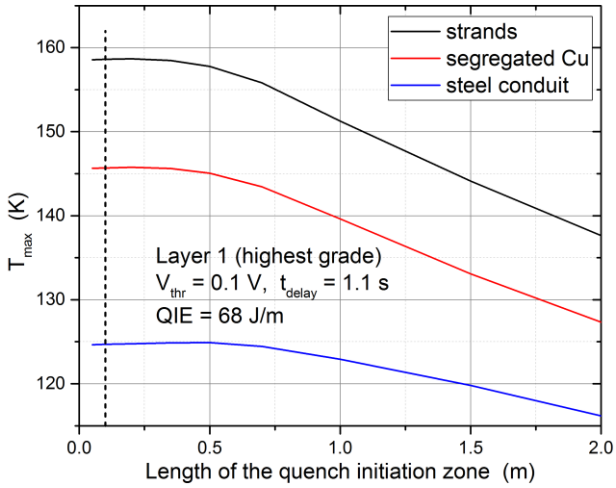

Fig. 9. Dependence of hot-spot temperature in layer 1 on the length of the quench initiation zone. The quench initiation energy was 68 J/m multiplied by the length of the quench initiation zone.

5. Conclusions

The thermo-hydraulic analysis of the react&wind DEMO TF conductors proposed by SPC in 2016 shows that the quench hot-spot temperature is safely below the acceptable limit of 150 K specified for the steel conduit. The hot-spot temperature strongly depends on the detection voltage threshold, V_{thr}, and on the delay time needed for quench validation and breakers opening. On the other hand, the hot-spot temperature is almost insensitive to the quench initiating energy. Also the length of quench initiation zone may affect the hot-spot temperature to some extent.

Acknowledgments

This work has been carried out within the framework of the EUROfusion Consortium and has received funding from the Euratom research and training programme 2014-2018 under grant agreement No 633053. The views and opinions expressed herein do not necessarily reflect those of the European Commission.

This scientific work was also partly supported by Polish Ministry of Science and Higher Education within the framework of the scientific financial resources in the year 2016 allocated for the realization of the international co-financed project.

References

[1] L. Zani et al., Overview of Progress on the EU DEMO Reactor Magnet System Design, IEEE Trans. Appl. Supercond., vol. 24, Article no. 4204505, 2016.

[2] K. Sedlak et al., Design and R&D for the DEMO Toroidal Field Coils based on Nb_3Sn React and Wind Method, ASC conference 2016, submitted to IEEE Trans. Appl. Supercond.

[3] M. Lewandowska, K. Sedlak, L. Zani, Thermal-Hydraulic Analysis of the Low-T-c Superconductor (LTS) Winding Pack Design Concepts for the DEMO Toroidal Field (TF) Coil, IEEE Trans. Appl. Supercond., vol. 26, Article no. 4205305, 2016.

[4] M. Lewandowska, K. Sedlak, Thermal-hydraulic analysis of the improved LTS conductor design concepts for the DEMO TF coil, Prz. Elektrotech., vol. 92, no. 4, pp. 179–182, 2016.

[5] M. Lewandowska, K. Sedlak, L. Zani, Thermal-Hydraulic Analysis of LTS Cables for the DEMO TF Coil, IEEE Trans. Appl. Supercond., vol. 24, Article no. 4200305, 2016.

[6] M. Lewandowska, A. Dembkowska, Thermal – hydraulic analysis of LTS cables for the DEMO TF coil using simplified models, presented at 13th Kudowa Summer School 2016, submitted to Nukleonika.

[7] R. Zanino et al., Development of a Thermal-Hydraulic Model for the European DEMO TF Coil, IEEE Trans. Appl. Supercond., vol. 26, Article no. 4201606, 2016.

[8] R. Vallcorba et al., Thermo-hydraulic analyses associated with a CEA design proposal for a DEMO TF conductor, Cryogenics, in print, 2016.

[9] B. Stepanov, P. Bruzzone, DEMO-EUROfusion Tokamak, Design of TF Coil Inter-layer Splice Joint, SOFT 2016 conference, submitted to Fus. Eng. Des.

[10] L. Bottura, C. Rosso, M. Breschi, A general model for thermal, hydraulic and electric analysis of superconducting cables, Cryogenics, vol. 40, pp. 617–626, 2000.

[11] M. Bagnasco, L. Bottura and M. Lewandowska, Friction factor correlation for CICC's based on a porous media

analogy, Cryogenics, vol. 50, p. 711–719, 2010.
[12] R. Shah and D. Sekulić, Fundamentals of Heat Exchanger Design, New Jersey: Wiley, 2003.
[13] L. Savoldi et al., Common approach for thermal-hydraulic calculations. [Online]. Available: https://idm.euro-fusion.org/?uid=2LMECE.
[14] K. Sedlak et al., Common operating values for DEMO magnets design for 2016. [Online]. Available: https://idm.euro-fusion.org/?uid=2MMDTG.